Macromolecules

pubs.acs.org/Macromolecules Article

Poly(cyclosilane) Postpolymerization Hydrosilylation

Marissa G. Coschigano, Sydney L. Gregory, Jonathan Catazaro, Aaron J. Rossini, and Rebekka S. Klausen*

Cite This: https://doi.org/10.1021/acs.macromol.3c02110 Read Online

ACCESS | Metrics & More | Article Recommendations | Supporting Information

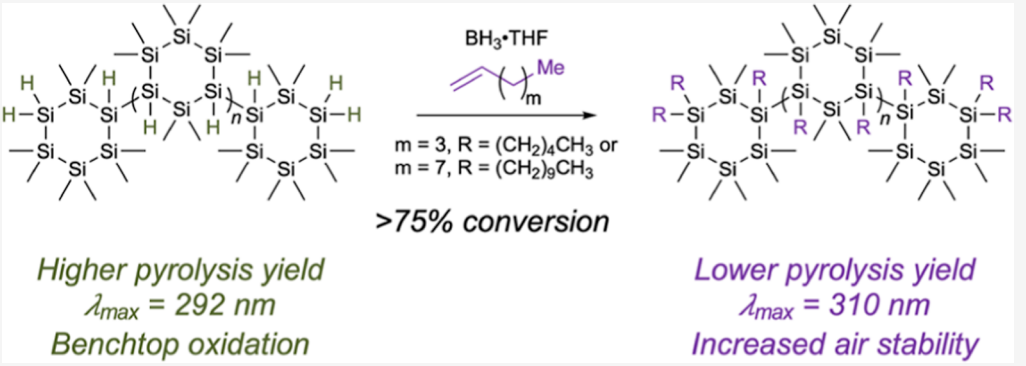

ABSTRACT: Postpolymerization functionalization is a key strategy in the diversification of polymeric materials for the conferral of tailored properties. Poly(cyclosilane)s are structurally complex polymers with an all-silicon backbone, featuring a periodic array of hydrido (Si−H) side chains that are potentially suitable for postpolymerization functionalization via hydrosilylation. At the same time, classical methods for hydrosilylation employing Pt- or Pd-based catalysts can result in Si−Si bond scission. Herein, we demonstrate borane-catalyzed hydrosilylation reactions between α-olefins and small molecules or three distinct poly(cyclosilane) architectures. We investigate chemoselectivity for end group versus internal Si−H groups and find that ^{29}Si cross-polarization magic angle spinning can provide insight on site-selectivity in the functionalization of a complex poly(cyclosilane). We further show that postpolymerization hydrosilylation, converting oxidatively sensitive Si−H groups to Si−alkyl chains, modulates solubility and physical characteristics, optical properties, pyrolytic reactivity, and air sensitivity.

1. INTRODUCTION

While polysilanes, organometallic polymers with the general formula poly(SiR_2),[1] have been known almost as long as organic polymers, their structural diversity lags behind that of polyolefins, which limits insight into structure−property relationships.[2,3] Reasons for this knowledge gap include the more limited pool of reactive silane monomers,[4] the low functional group tolerance of Wurtz coupling, the most widely used synthetic approach to polysilanes,[5] as well as challenges in structural characterization, which has, for example, complicated assignment of polysilane tacticity.[6−8]

Postpolymerization functionalization has emerged as a key tool for the introduction of structural diversity into polysilanes, with early examples focusing on dearylation of polyphenylsilanes with acetyl chloride/aluminum chloride or triflic acid.[9−12] The development of dehydropolymerization of trihydrosilanes ($RSiH_3$)[13,14] giving rise to hydrido-functionalized polymers of the general structure poly(SiHR) suggested the possibility of Si−H activation for postpolymerization functionalization. Examples include free radical-initiated chlorination of Si−H bonds,[15] dimethyltitanocene-mediated Si−H/N−H dehydrocoupling,[16] and $AlCl_3$-promoted hydrosilylation.[17] In all of these reactions, some Si−Si backbone cleavage competed with Si−H side chain activation. However, as documented by Rosenberg, the Lewis acid tris(pentafluorophenyl)borane ($B(C_6F_5)_3$) exhibits high chemoselectivity for Si−H over Si−Si bonds while also facilitating the coupling of poly(SiHPh) to a broad range of partners including thiols,[18,19] thioketones,[20] ketones,[20] and alkynes.[20]

In recent years, we have focused on the synthesis and dehydropolymerization of cyclosilane monomers[21] as a route to increasing structural complexity in polymeric materials derived from Group 14, resulting in the family of poly(cyclosilane)s (Figure 1a).[4] Examples of structural control include the determination of linear or cyclic architecture,[22,23] degree of branching,[24] and new forms of tacticity.[25,26] Recently, we have achieved greater insight into the relationship

Received: October 13, 2023
Revised: April 2, 2024
Accepted: April 9, 2024

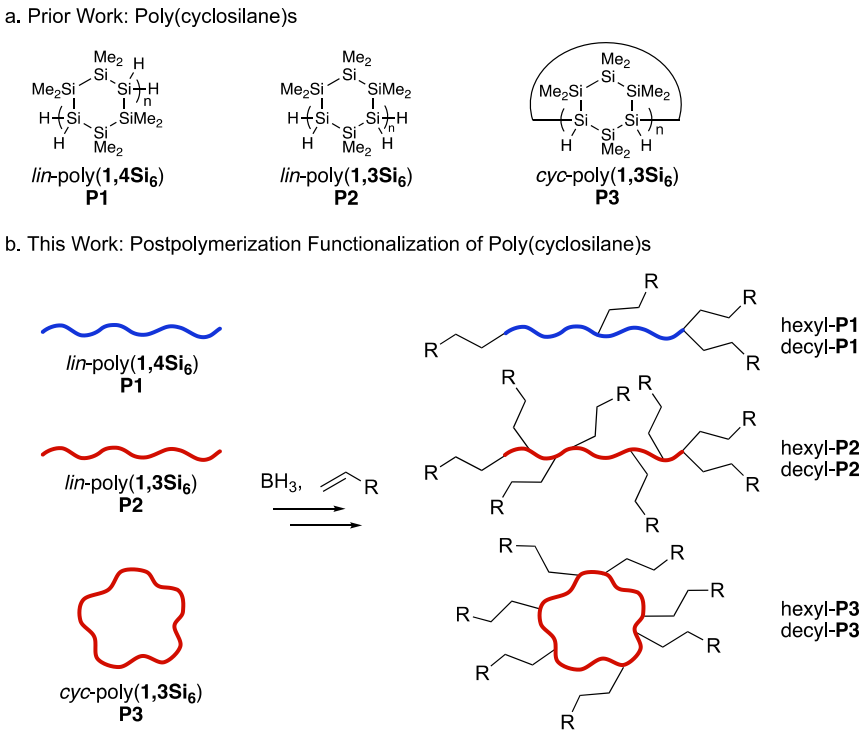

Figure 1. (a) Prior work: synthesis of poly(cyclosilane)s. (b) This work: postpolymerization functionalization of poly(cyclosilanes) via catalytic hydrosilylation.

Scheme 1. (a) Inequivalent Chemical Environments of a Typical Poly(cyclosilane). (b) Molecular Models for poly(Cyclosilane)s. (c) Reaction Conditions and Possible Functionalization Outcomes, m = 3

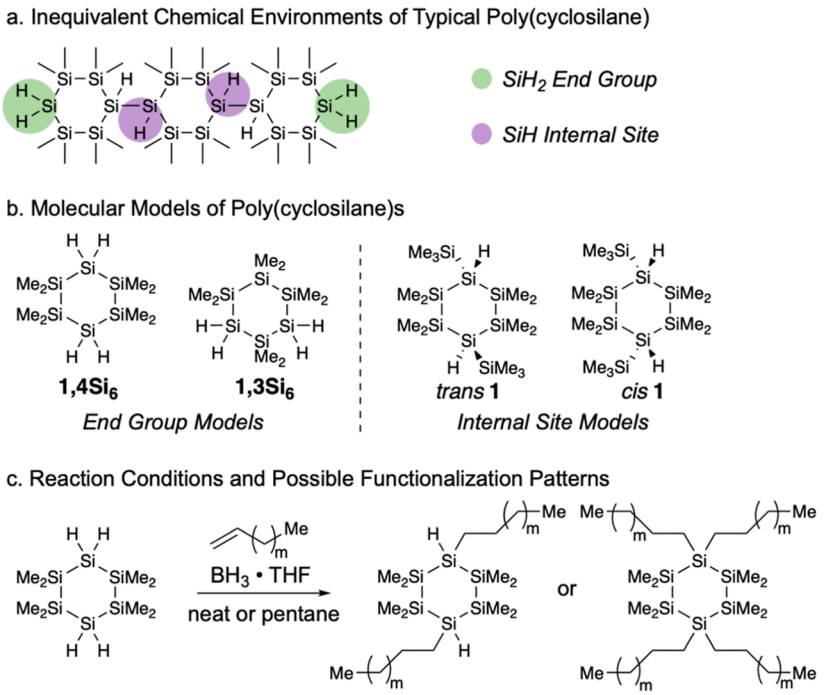

between poly(cyclosilane) microstructure and physical properties, including thermal behavior and pyrolysis[27] and absorbance spectra.[28]

We became interested in the possibility of postpolymerization functionalization of the poly(cyclosilane)s. Exhaustive replacement of the Si−H bonds with inert long-chain alkyl groups (e.g., hexyl) might confer greater solubility and processability, while also impacting pyrolytic reactivity toward the synthesis of polymer-derived ceramics.[29] Given prior work that Si−H bonds initiate autoxidation and decomposition of poly(SiHPh),[30] we also considered if Si−H to Si−R replacement might impact air stability. We therefore envisioned a hydrosilylation reaction between a poly(cyclosilane) and a terminal alkene (Figure 1b). However,

https://doi.org/10.1021/acs.macromol.3c02110
Macromolecules XXXX, XXX, XXX−XXX

previously reported polysilane Si−H functionalization reactions with terminal alkenes did not proceed to high conversion (e.g., 1-hexene/poly(SiHPh)/$B(C_6F_5)_3$ = 40% conversion).[20]

Hydrosilylation is also a critical reaction for the functionalization of silicon surfaces and nanostructures.[31,32] In particular, we were interested in a report by Veinot et al. on borane [BH_3·tetrahydrofuran (THF)] to mediate hydrosilylation reactions between H-terminated silicon nanoparticles and simple alkenes, which proceeded to high degrees of conversion based on Fourier transform infrared (FTIR) analysis.[33] At the same time, we appreciated that the greater structural complexity of the poly(cyclosilane)s relative to that of an H-terminated silicon nanoparticle might prove to be a challenge for postpolymerization functionalization. For example, poly(cyclosilane)s possess several inequivalent Si−H environments (Scheme 1a) differing in steric crowding and electronic activation.

Herein, we report that postpolymerization functionalization of the poly(cyclosilane)s via borane-catalyzed hydrosilylation typically proceeds to high conversion without backbone scission, yielding polysilanes readily dispersed or swelled in organic solvents. Extensive model studies on small-molecule systems support the possibility of achieving high degrees of functionalization. ^{29}Si cross-polarization magic angle spinning (CPMAS) spectroscopy enabled the structural assignment of site-selectivity between end-group and internal side chain hydridos. The failure of size exclusion chromatography (SEC) to accurately assess poly(cyclosilane) functionalization is also described. We report that attachment of long chain alkanes to the poly(cyclosilane) scaffold confers not only increased solubility but also differences in pyrolytic reactivity and UV−vis absorbance.

2. EXPERIMENTAL SECTION

2.1. Methods and Materials. Unless otherwise specified, all chemicals were used and purchased without further purification. Solvents dichloromethane (DCM) (Sigma-Aldrich, HPLC grade) and pentane (Fischer, certified ACS) were dried on a J. C. Meyer solvent dispensing system using stainless-steel columns packed with neutral alumina (except for toluene, which is dried with neutral alumina and Q5 reactant, a copper(II) oxide oxygen scavenger), following the manufacturer's recommendations for solvent preparation and dispensation, unless otherwise noted. Methanol (Sigma-Aldrich, HPLC grade) was degassed via freeze−pump−thaw methodology to be used in the glovebox. Xylene was purchased from Acros Organics; 1-hexene, 1-decene, and borane THF complex solution (BH_3, 1 M in THF) were purchased from Sigma-Aldrich. Cyclosilanes *cis*- and *trans*-1,4-bis(trimethylsilyl)-1,4-dihydro-octamethylcyclohexasilanes (*trans*- and *cis*-**1**) were synthesized according to an adaptation of the literature procedure.[34] Poly(cyclosilane)s *lin*-poly(**1,4Si$_6$**), *lin*-poly(**1,3Si$_6$**), and *cyc*-poly(**1,3Si$_6$**) were synthesized via dehydro-coupling polymerization of bifunctional monomers (**1,4Si$_6$** and **1,3Si$_6$**) according to the literature procedure.[22,23,27]

Solution-phase ^{1}H NMR, ^{13}C {^{1}H} NMR, and ^{29}Si {^{1}H} NMR spectra were recorded on either a Bruker AVANCE 300 or 400 MHz spectrometer or a Bruker AVANCE III HD 400 MHz spectrometer, and chemical shifts are reported in parts per million (ppm). Spectra were recorded in benzene-d_6 with the residual solvent peak as the internal standard (^{1}H NMR: C_6H_6 δ = 7.16). Solid-state ^{1}H NMR, ^{13}C {^{1}H} NMR, and ^{29}Si {^{1}H} NMR spectra were recorded on a Bruker Ascend 500 MHz spectrometer with a Bruker 4.0 mm iProbe and AVANCE NEO console. A RAMP-CP Hartman-Hahn pulse program with the ramp centered on a matching sideband, 5.8 μs ^{1}H 90° pulse, 114.53 W (of a 140 W 100% power total), 10 kHz MAS frequency, and ∼11 h acquisition time (8000−20 000 scans) were used. ^{1}H heteronuclear decoupling was performed with the TPPM pulse sequence with a ^{1}H RF field of 90 kHz.[35] CP contact times were optimized on each sample to maximize signal intensity and were between 2.5 and 4.0 ms. For select samples, we also tested the multiCP pulse sequence. For the multiCP pulse sequence, we used three CP steps that were each 8.0 ms in duration. The time between CP steps was 5.0 s. All chemical shifts are reported in ppm. All samples were packed into a 4.0 mm zirconia rotor in a glovebox under a nitrogen atmosphere. Dry nitrogen gas was used for all of the MAS experiments. Molecular weights were measured by gel permeation chromatography (GPC) on a Tosoh Bioscience EcoSEC GPC workstation with UV detection at 254 nm using butylated hydroxytoluene stabilized THF as the eluent (0.35 mL min^{-1}, 40 °C) through a TSKgel SuperMultipore HZ-M guard column (4.6 mm ID ⊆2.0 cm, 4 μm, Tosoh Bioscience). Polystyrene standards (EasiVial PS-M, Agilent) were used to build the calibration curve. Processing was performed using EcoSEC Data Analysis software (Version 1.14, Tosoh Bioscience). The samples were dissolved in THF (1 mg mL^{-1}), filtered through syringe filters (Millex-FG Syringe Filter Unit, 0.20 μm, PTFE, EMD Millipore), and injected by an autosampler (10 μL). High-resolution mass spectrometry (HRMS) was performed in the Department of Chemistry at Johns Hopkins University using a VG Instruments VG70S/E magnetic sector mass spectrometer with electron ionization (EI) (70 eV). The UNIlab Plus Glove Box by MBRAUN was maintained under a nitrogen atmosphere. All column chromatography experiments were performed on a Teledyne ISCO CombiFlash Rf + using RediSep Rf silica columns. IR spectra were collected on a Thermo Scientific Nicolet iS5 spectrometer equipped with an iD5 ATR laminated diamond crystal attachment. Thermogravimetric analysis (TGA) was conducted using a TA Instruments SDT Q600 under flowing Ar at a heating rate of 5.0 °C min^{-1} from 40 to 600 °C. UV−vis spectra were collected on a Varian Cary 50 Bio UV−vis spectrophotometer, dissolved in non-UV stabilized THF in 1 cm quartz cuvettes.

2.1.1. General Procedure for Cyclosilane Hydrosilylation. In an inert atmosphere glovebox, a 10 mL Schlenk flask equipped with a stir bar was charged with cyclosilane (1.0 equiv). The flask was sealed, removed from the glovebox, and attached to the Schlenk line. The cyclosilane was dissolved in 1-hexene (3.0 or 40.0 equiv). The reaction mixture was cooled to 0 °C by submerging the reaction vessel in an ice water bath. BH_3·THF (4 or 2 mol % with respect to alkene) was added via a syringe, and the solution was stirred while allowing the bath to warm to room temperature. After 48 h, the excess alkene was removed under vacuum on the Schlenk line at room temperature overnight. Automated column chromatography with 100% hexanes yielded the hydrosilylation product.

*2.1.1.1. Synthesis of **2** from **1,4Si$_6$** and 1-Hexene.* The general procedure was followed employing **1,4Si$_6$** (1.0 equiv, 0.342 mmol, 100 mg), 1-hexene (40.0 equiv, 13.68 mmol, 1.7 mL), and BH_3·THF (0.8 equiv, 0.274 mmol, 0.27 mL, 1 M in THF). The crude product, a colorless oil, was purified by automated column chromatography with 100% hexanes to yield **2** as a colorless oil after removal of the solvent (yield: 190 mg, 88%). ^{1}H NMR (C_6D_6, δ ppm): 1.64−1.52 (m, 9H), 1.50−1.40 (m, 12H), 1.39−1.27 (m, 18H), 1.05−0.97 (m, 9H), 0.97−0.89 (m, 12H), 0.41 (s, 24H). ^{13}C {^{1}H} NMR (C_6D_6, δ ppm): 33.9, 31.6, 27.2, 22.8, 14.0, 11.6, −4.6. ^{29}Si {^{1}H} NMR (C_6D_6, δ ppm) 35.7, 41.8. HRMS calcd for $C_{32}H_{76}Si_6$, 628.4563; found, 628.45609.

*2.1.1.2. Synthesis of **3** from **1,3Si$_6$** and 1-Hexene.* The general procedure was followed employing **1,3Si$_6$** (1.0 equiv, 0.342 mmol, 100 mg), 1-hexene (40.0 equiv, 13.68 mmol, 1.7 mL), and BH_3·THF (0.8 equiv, 0.274 mmol, 0.27 mL, 1 M in THF). The crude product, a colorless oil, was purified by automated column chromatography with 100% hexanes to yield **3** as a colorless oil after removal of the solvent (yield: 200 mg, 93%). ^{1}H NMR (C_6D_6, δ ppm): 1.63−1.50 (m, 9H), 1.48−1.38 (m, 12H), 1.37−1.27 (m, 18H), 1.04−0.96 (m, 9H), 0.94−0.86 (m, 12H), 0.42 (s, 6H), 0.34 (s, 12H), 0.27 (s, 6H). ^{13}C {^{1}H} NMR (C_6D_6, δ ppm): 34.0, 31.7, 27.2, 22.8, 14.0, 11.6, −2.9, −4.5, −6.2. ^{29}Si {^{1}H} NMR (C_6D_6, δ ppm) 35.5, 41.6. HRMS calcd for $C_{32}H_{76}Si_6$, 628.4563; found, 628.45608.

*2.1.1.3. Synthesis of **4** from trans-**1** and 1-Hexene.* The general procedure was followed with the following modification: *trans*-**1** (1.0

https://doi.org/10.1021/acs.macromol.3c02110
Macromolecules XXXX, XXX, XXX−XXX

Scheme 2. Results of Borane-Catalyzed Hydrosilylation of Molecular Models. Diastereomeric Ratio of 4 Was Not Determined. Catalyst Loading of BH_3·THF Reported with Respect to the Alkene

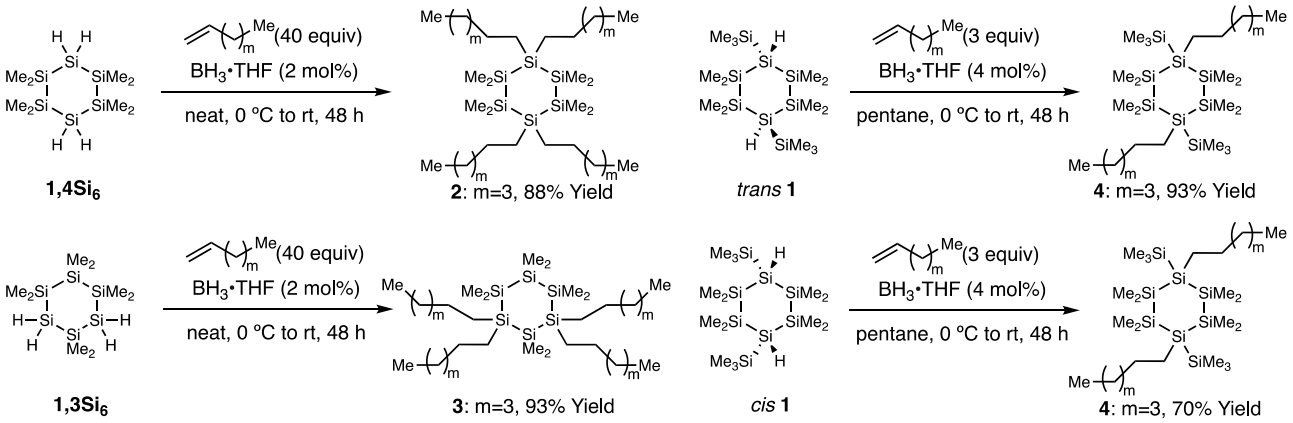

equiv, 0.229 mmol, 100 mg) was diluted in anhydrous pentane (0.5 mL) before the addition of 1-hexene (3.0 equiv, 0.686 mmol, 0.09 mL) and BH_3·THF (0.11 equiv, 0.026 mmol, 26 μL, 1 M in THF). The crude product, a white solid, was purified by automated column chromatography with 100% hexanes to yield **4** as a white solid after removal of the solvent (yield: 129 mg, 93%). ^{1}H NMR (C_6D_6, δ ppm): 1.62−1.51 (m, 4H), 1.45−1.37 (m, 4H), 1.35−1.28 (m, 9H), 1.09−1.00 (m, 4H), 0.93−0.86 (m, 8H), 0.40 (s, 18H), 0.32 (s, 16H). ^{13}C {^{1}H} NMR (C_6D_6, δ ppm): 34.2, 31.5, 29.9, 22.7, 14.0, 10.0, 2.2, −2.4. ^{29}Si {^{1}H} NMR (C_6D_6, δ ppm): −9.7, −37.8, −75.1. HRMS calcd for $C_{26}H_{68}Si_8$, 604.3474; found, 604.3475.

*2.1.1.4. Synthesis of **4** from cis-**1** and 1-Hexene.* The general procedure was followed with the following modification: *cis*-**1** (1.0 equiv, 0.229 mmol, 100 mg) was diluted in anhydrous pentane (0.5 mL) before the addition of 1-hexene (3.0 equiv, 0.686 mmol, 0.09 mL) and BH_3·THF (0.11 equiv, 0.026 mmol, 26 μL, 1 M in THF). The crude product, a colorless oil, was purified by automated column chromatography with 100% hexanes to yield **4** as a colorless oil after removal of the solvent (yield: 96 mg, 70%). ^{1}H NMR (C_6D_6, δ ppm): 1.63−1.51 (m, 4H), 1.46−1.37 (m, 4H), 1.37−1.26 (m, 9H), 1.09−0.99 (m, 4H), 0.94−0.86 (m, 8H), 0.40 (s, 18H), 0.32 (s, 16H). ^{13}C {^{1}H} NMR (C_6D_6, δ ppm): 34.1, 31.5, 29.9, 22.7, 14.0, 10.0, 2.2, −3.5. ^{29}Si {^{1}H} NMR (C_6D_6, δ ppm): −9.7, −37.8, −75.2. HRMS calcd for $C_{26}H_{68}Si_8$, 604.3474; found, 604.3483.

2.1.2. General Procedure for Oxidation. A 10 mL round-bottomed flask equipped with a stir bar was charged with 50 mg of a cyclosilane (0.085−0.170 mmol), which was dissolved in xylenes (85 mM). The flask was fitted with a vented reflux condenser and heated at 183 °C for 24 h. No further purification was conducted.

2.1.3. General Procedure for Poly(cyclosilane) Hydrosilylation. In an inert atmosphere glovebox, a 10 mL Schlenk flask equipped with a stir bar was charged with polymer. The flask was sealed, removed from the glovebox, and attached to the Schlenk line. The cyclosilane was dissolved in alkene (1-hexene or 1-decene, 10 equiv with respect to calculated number of SiH bonds). The reaction mixture was cooled to 0 °C by submerging the reaction vessel in an ice water bath. BH_3·THF (2 mol % with respect to alkene) was added via a syringe, and the solution was stirred while allowing the bath to warm to room temperature. After 48 h, the excess alkene was removed under vacuum on the Schlenk line at room temperature overnight. Precipitation of the crude product dissolved in minimal DCM in methanol yielded the hydrosilylation product.

*2.1.3.1. Synthesis of Hexyl-**P1** from lin-poly(**1,4Si$_6$**) and 1-Hexene.* The general procedure was followed employing *lin*-poly(**1,4Si$_6$**) (1.0 equiv, 0.075 mmol, 207 mg), 1-hexene (209 equiv, 15.69 mmol, 1.96 mL), and BH_3·THF (4.1 equiv, 0.31 mmol, 0.31 mL, 1 M in THF). The crude product, a white solid, was purified by precipitation into methanol to yield hexyl-**P1** as a white solid after filtration and removal of the solvent (yield: 148 mg, 33%). ^{13}C {^{1}H} NMR (δ ppm): 35.03, 32.00, 23.46, 14.81, 2.95, −2.18. ^{29}Si {^{1}H} NMR (δ ppm): 24.28 to 15.94 (0.08Si), −19.97 to −39.81 (4Si), −47.84 to −58.85 (0.30Si), −88.80 to −93.85 (0.03Si), −101.88 to −116.43 (1.73Si).

*2.1.3.2. Synthesis of Decyl-**P1** from lin-poly(**1,4Si$_6$**) and 1-Decene.* The general procedure was followed employing *lin*-poly(**1,4Si$_6$**) (1.0 equiv, 0.045 mmol, 125 mg), 1-decene (210 equiv, 9.46 mmol, 1.79 mL), and BH_3·THF (4.2 equiv, 0.19 mmol, 0.19 mL, 1 M in THF). The crude product, a white solid, was purified by precipitation into methanol to yield decyl-**P1** as a white solid after filtration and removal of the solvent (yield: 104 mg, 48%). ^{13}C {^{1}H} NMR (δ ppm): 34.82, 32.72, 30.26, 23.50, 14.77, 2.90, −2.30. ^{29}Si {^{1}H} NMR (δ ppm): 23.49 to 6.88 (0.29Si), −20.50 to −41.14 (4Si), −50.25 to −59.65 (0.24Si), −88.57 to −94.79 (0.05Si), −100.12 to −118.38 (2.41Si).

*2.1.3.3. Synthesis of Hexyl-**P2** from lin-poly(**1,3Si$_6$**) and 1-Hexene.* The general procedure was followed employing *lin*-poly(**1,3Si$_6$**) (1.0 equiv, 0.048 mmol, 84 mg), 1-hexene (140 equiv, 6.71 mmol, 0.76 mL), and BH_3·THF (2.7 equiv, 0.13 mmol, 0.13 mL, 1 M in THF). The crude product, a colorless oil, was purified by precipitation into methanol to yield hexyl-**P2** as a white solid after filtration and removal of the solvent (yield: 58 mg, 34%). ^{13}C {^{1}H} NMR (δ ppm): 34.53, 31.92, 30.62, 23.30, 14.68, 2.48, −1.60. ^{29}Si {^{1}H} NMR (δ ppm): 27.23 to 12.16 (0.33Si), −13.57 to −36.67 (4Si), −39.85 to −60.20 (1.08Si), −82.19 to −91.87 (0.03Si), −93.52 to −113.10 (0.32Si).

*2.1.3.4. Synthesis of Decyl-**P2** from lin-poly(**1,3Si$_6$**) and 1-Decene.* The general procedure was followed employing *lin*-poly(**1,3Si$_6$**) (1.0 equiv, 0.071 mmol, 139 mg), 1-decene (154 equiv, 10.94 mmol, 2.07 mL), and BH_3·THF (3.10 equiv, 0.22 mmol, 0.22 mL, 1 M in THF). The crude product, a colorless oil, was purified by precipitation into methanol to yield decyl-**P2** as a viscous colorless oil after filtration and removal of the solvent (yield: 148 mg, 70%).

*2.1.3.5. Synthesis of Hexyl-**P3** from Cyc-poly(**1,3Si$_6$**) and 1-Hexene.* The general procedure was followed employing *cyc*-poly(**1,3Si$_6$**) (1.0 equiv, 0.050 mmol, 172 mg), 1-hexene (234 equiv, 11.70 mmol, 1.46 mL), and BH_3·THF (4.6 equiv, 0.23 mmol, 0.23 mL, 1 M in THF). The crude product, a colorless oil, was purified by precipitation into methanol to yield hexyl-**P3** as a white solid after filtration and removal of the solvent (yield: 142 mg, 80%). ^{13}C {^{1}H} NMR (δ ppm): 34.69, 31.85, 23.55, 14.75, 2.21, −1.77. ^{29}Si {^{1}H} NMR (δ ppm): −12.84 to −38.99 (4Si), −39.20 to −63.71 (1.12Si), −85.79 to −118.42 (0.59Si).

*2.1.3.6. Synthesis of Decyl-**P3** from Cyc-poly(**1,3Si$_6$**) and 1-Decene.* The general procedure was followed employing *cyc*-poly(**1,3Si$_6$**) (1.0 equiv, 0.037 mmol, 135 mg), 1-decene (270 equiv, 10.00 mmol, 1.89 mL), and BH_3·THF (5.4 equiv, 0.20 mmol, 0.20 mL, 1 M in THF). The crude product, a colorless oil, was purified by precipitation into methanol to yield decyl-**P3** as a viscous

https://doi.org/10.1021/acs.macromol.3c02110
Macromolecules XXXX, XXX, XXX−XXX

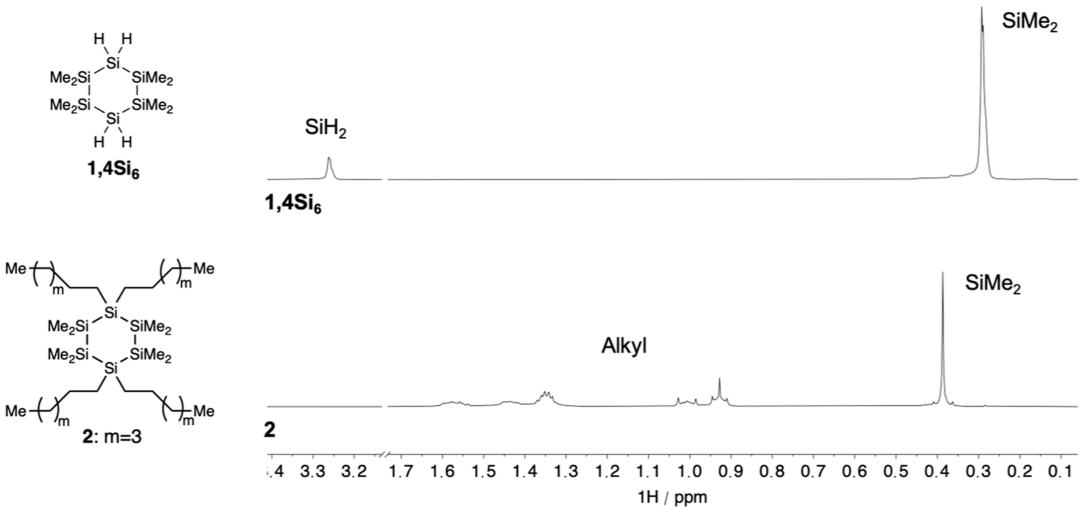

Figure 2. ^{1}H NMR (400 MHz, C_6D_6) spectra of **1,4Si$_6$** and **2** show no cleavage of Si−Si bonds.

Scheme 3. Postpolymerization Functionalization of Poly(cyclosilane)s P1, P2, and P3. The Products Are Shown as 100% Functionalized. Catalyst Loading of BH_3·THF Reported with Respect to the Alkene

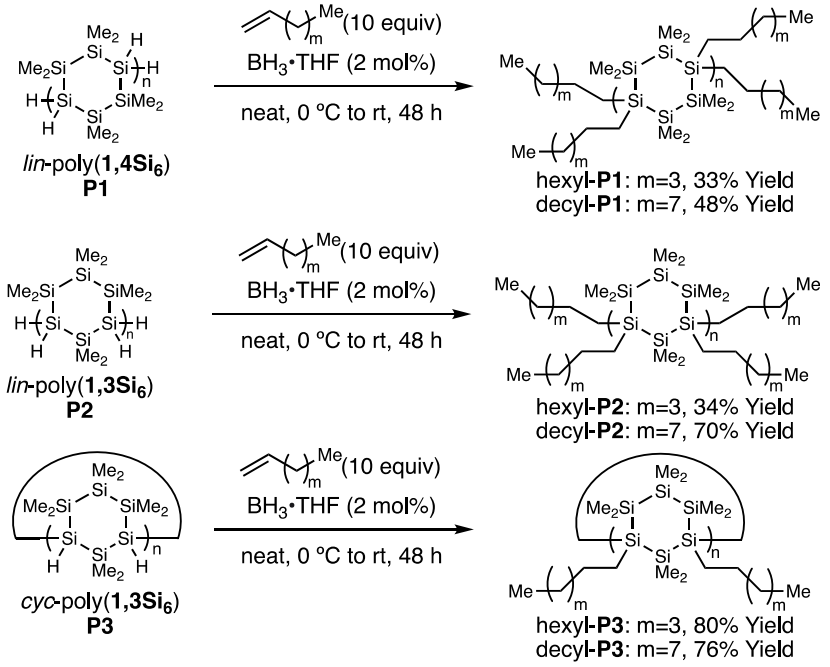

colorless oil after filtration and removal of solvent (yield: 138 mg, 76%).

3. RESULTS AND DISCUSSION

3.1. Hydrosilylation Reactions between α-Olefins and Small Molecules. In their original report, Veinot et al. showed that several terminal alkenes including 1-pentene, 1-octene, and 1-decene were effective in silicon nanocrystal functionalization.[33] As mentioned above, we appreciated that the poly(cyclosilane)s differed significantly in structure from a nanocrystal in terms of having multiple inequivalent chemical environments (Scheme 1a). In addition, competitive Si−Si cleavage over Si−H activation might be more significant in a linear polymer than in a nanocrystal.

To test the effectiveness of borane-catalyzed hydrosilylation on cyclosilanes as well as the possibility of Si−Si scission, several small molecules were chosen as probes of the potential reactivity of the poly(cyclosilane)s (Scheme 1b). The cyclosilane monomers **1,4Si$_6$** and **1,3Si$_6$** were used to represent the end groups of the linear polymers. The compounds *cis*- and *trans*-**1**[34] were chosen to represent the Si−H internal site chemical environment. Both *cis*- and *trans*-**1** were employed to examine the potential impact of tacticity, as poly(cyclosilane)s possess *cis/trans* stereoisomerism.[26] We were also interested in whether addition would proceed once or twice at each SiH_2 site, giving rise to either di- or tetra-alkyl cyclosilanes (Scheme 1c). Prior work from our group on Ru-catalyzed hydrosilylation reactions of SiH_2-functionalized cyclosilanes and phenylacetylene resulted in exclusive difunctionalization (e.g., SiHR).[25]

Using excess 1-hexene and 2 or 4 mol % BH_3·THF, we tested the efficacy of borane-catalyzed hydrosilylation (Scheme 2). All reactions were monitored by ^{1}H NMR spectroscopy. The disappearance of peaks assigned to the Si−H sites (based

https://doi.org/10.1021/acs.macromol.3c02110
Macromolecules XXXX, XXX, XXX−XXX

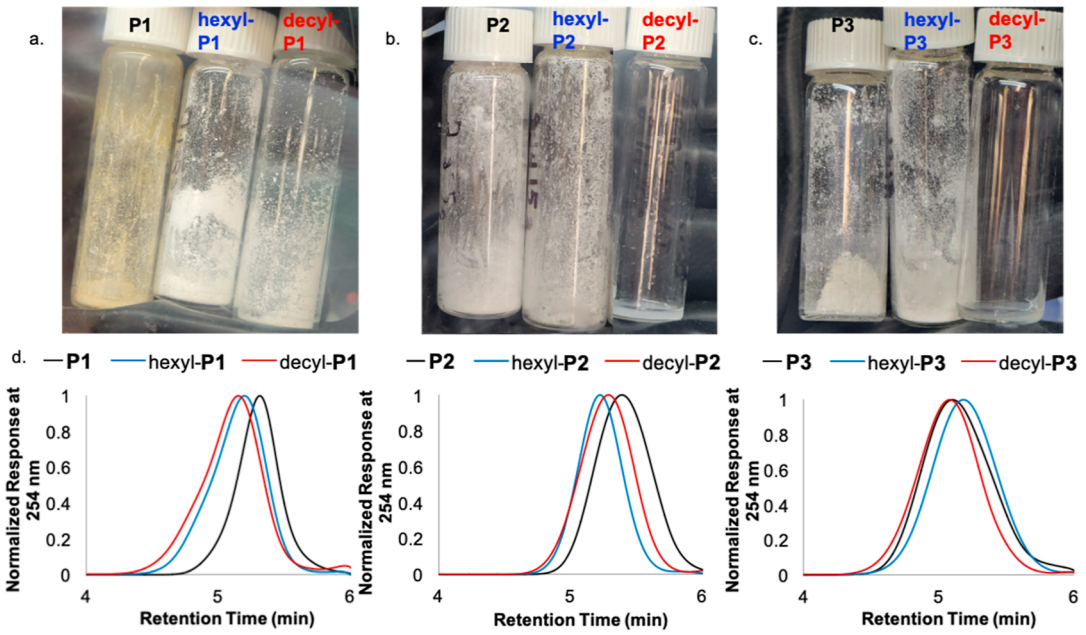

Figure 3. (a–c) Poly(cyclosilane)s before and after hydrosilylation. (d) Normalized GPC curves of **P1**–**3** and the alkylated variants.

on prior work)[20,22,23,26] and appearance of peaks assigned to alkyl C–H bonds was observed, consistent with the formation of products **2**–**4** (Figures 2, S1–S3). In the case of **1,3Si$_6$**, we also identified structural signatures of partially alkylated intermediates, and mass spectroscopy data were also consistent with partially alkylated intermediates (see Supporting Information). No evidence of significant Si–Si cleavage was identified as the distinct sharp $SiMe_2$ features were retained, consistent with the symmetry of a cyclic compound. High yields (70–93%) were obtained. Retention of the relative configuration of the starting material was not observed in the hydrosilylation reactions of *cis*- and *trans*-**1** with 1-hexene, which may support Veinot's proposal of a silylium ion intermediate in their original work on nanocrystal surface functionalization.[33]

These data indicate that borane is an effective catalyst for the comprehensive functionalization of both secondary and tertiary silanes without competitive Si–Si scission. High-resolution EI mass spectrometry and ^{29}Si NMR spectra were also fully consistent with the assigned structures (see Supporting Information).

3.2. Hydrosilylation Reactions between α-Olefins and Poly(cyclosilane)s. Based on the molecular models described above, we hypothesized that postpolymerization functionalization of the poly(cyclosilane)s should occur at both internal Si–H and end group SiH_2 sites without fracturing the polymer backbone.

The hydrosilylation reaction conditions were adapted to poly(cyclosilane)s **P1**, **P2**, and **P3** (Scheme 3 and Table S1). We found that increasing the amount of BH_3 resulted in higher conversions (Table S1). Hydrosilylations were performed in neat alkene, with the dropwise addition of BH_3·THF (2 mol % with respect to alkene) at 0 °C, after which the reaction was allowed to warm to room temperature and continue for 48 h.

Lower yields were observed for hexyl- and decyl-**P1** due to the poor solubility of the starting material. Lower yields for hexyl-**P2** were attributed to decreased precipitation efficiency in the antisolvent.

After hydrosilylation, we observed changes in the appearance and physical properties of the polymers (Figure 3a–c). For example, hexyl-**P2** was isolated as a white solid and decyl-**P2** was isolated as a colorless viscous oil (Figure 3b), while **P2** itself is a white glassy solid. We also observed an increase in the solubility of hexyl-**P1** compared to that of **P1** itself as the hydrosilylation reaction progressed (Figure S4).

Changes in the molecular weight characteristics were monitored by GPC analysis (Table 1, Figure 3d). For **P1** and **P2**, after hydrosilylation, a shift to a shorter retention time and an increase in M_n were observed compared to that observed in the parent polymer, which is consistent with an increase in the hydrodynamic radius and molecular weight reflecting the addition of longer side chains. **P3** was anomalous in not showing a straightforward shift to higher M_n after hydrosilylation, which is discussed further below.

Table 1. Molecular Weight Characteristics of Functionalized Poly(cyclosilane)s

polymer	M_n (g/mol)[a]	M_w/M_n
P1	2490	1.29
hexyl-**P1**	5910	1.41
decyl-**P1**	4810	1.46
P2	1860	1.37
hexyl-**P2**	3531	1.24
decyl-**P2**	2960	1.36
P3	4040	1.57
hexyl-**P3**	3560	1.55
decyl-**P3**	4920	1.49

[a]Determined by GPC relative to polystyrene standards at 254 nm (THF, [polymer] = 1 mg mL^{-1}, 40 °C, 0.35 mL min^{-1}, 10 μL injection).

The dispersity M_w/M_n remained ca. 1.3–1.5 for all samples, indicating that functionalization occurred without fragmenting the polymer backbone. We noted a slight shoulder peak for hexyl- and decyl-**P1** in comparison to that for **P1**, along with an increase in the solubility. We hypothesize that since **P1** is

https://doi.org/10.1021/acs.macromol.3c02110
Macromolecules XXXX, XXX, XXX–XXX

poorly soluble in the hydrosilylation reaction medium (1-hexene or 1-decene); as hydrosilylation proceeded and solubility increased, hydrosilylation could be accelerated for partially alkylated chains relative to **P1**, resulting in a nonuniform evolution in the molecular weight characteristics.

As mentioned above, the functionalization of **P3** did not follow the same trend as that of **P1** and **P2** of increasing M_n after hydrosilylation, which might suggest that hydrosilylation did not occur. However, the macrocyclic nature of **P3** may result in anomalous elution behavior and change in hydrodynamic radius as measured by GPC analysis.[36] For example, linear and cyclic polystyrene of the same degree of polymerization exhibit different retention times, as observed by gel permeation chromatography.[37] This limitation of GPC analysis does not allow for the degree of functionalization of macrocyclic **P3** to be measured based on molecular weight characteristics. Evidence that hydrosilylation did occur for **P3** could be obtained from FTIR spectroscopy. After the hydrosilylation reaction, we observed an intensification and increase in the number of resonances corresponding to C−H alkyl stretches (2900 cm^{-1}) along with a decrease in the intensity of the Si−H stretching frequency (2050 cm^{-1}) when comparing hexyl- and decyl-**P3** to **P3** (Figure 4). This trend was observed for hexyl- and decyl-**P1** and **P2** as well (Figures S5 and S6).

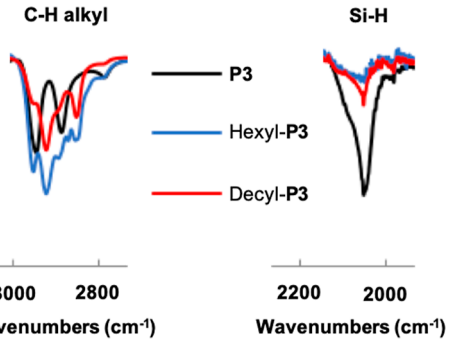

Figure 4. Cropped IR spectra of **P3**, hexyl-**P3**, and decyl-**P3**, highlighting the alkyl C−H (left) and Si−H (right) stretching frequencies.

3.3. Optimizing the ssNMR Parameters. To confirm the IR data showing that cyclic **P3** underwent significant hydrosilylation, given the ambiguous molecular weight changes observed by GPC, a different supporting method was needed. Solid-state NMR (ssNMR) spectroscopy is a powerful tool for molecular structural characterization of polymers.[38−40] Klausen et al. previously demonstrated ^{1}H and ^{29}Si ssNMR experiments for the characterization of the polysilane microstructure.[26] In that prior work, ^{1}H−^{29}Si refocused-INEPT solid-state NMR experiments were used to determine the number of attached protons to a silicon atom for each ^{29}Si NMR resonance in the monomer **1,4Si$_6$** and the polymer **P1**, enabling unambiguous assignment of peaks to an SiH_2 end group or an SiH internal site. Furthermore, ^{1}H−^{29}Si CPMAS ssNMR spectra were shown to offer nearly quantitative peak intensities. Integration of the peaks in ^{1}H−^{29}Si CPMAS ssNMR spectra resulted in an estimated degree of polymerization of 20, which was consistent with the measurements of the number-average degree of polymerization obtained by GPC. Integration also allowed the determination of tacticity, or the relative amounts of two stereoisomeric forms of **P1**, when coupled to computational models. These data support the accuracy of ^{29}Si CPMAS peak integrations and formed the basis of the NMR experiments employed herein to examine the evolution in the structure of the poly(cyclosilane)s after hydrosilylation. It is well-known from ^{1}H−^{13}C CPMAS ssNMR experiments on various organic molecules that errors in peak integrals can be on the order of 15% for contact times of 2 to 3 ms, and we expect similar errors in peak integrals here.[41]

For each glassy polymer (**P1**, hexyl-**P1**, decyl-**P1**, **P2**, hexyl-**P2**, **P3**, and hexyl-**P3**), we optimized both the CP ^{1}H and ^{29}Si spin-lock conditions and contact time to maximize the signal of all Si peaks, focusing on the prominent $SiMe_2$ peak. The contact time and CP conditions that gave the maximum signal intensity for each polymer were then used to acquire a high-quality ^{29}Si CPMAS spectrum that could be integrated. The optimized CP contact times were between 2.5 and 4.0 ms (Table 2). The ^{29}Si CPMAS spectra and integrations are shown in Figure 5. Decyl-**P2** and decyl-**P3** were omitted from Table 2 because these materials were oily, suggesting that they have high degrees of molecular mobility that will partly average ^{1}H−^{29}Si dipolar couplings that mediate the CP polarization transfers. Initial attempts at characterizing decyl-**P2** and decyl-**P3** by solution-phase ^{29}Si distortionless enhancement by polarization transfer NMR spectroscopy resulted in poor signal-to-noise ratios.

Table 2. Calculated Cross-Polarization Times and Approximate Percent Functionalization

polymer	cross-polarization contact time (ms)	approximate internal Si−H % functionalization[a]	approximate end group SiH_2 % functionalization[b]
hexyl-**P1**	4.0	15	73
decyl-**P1**	2.5	9	85
hexyl-**P2**	2.5	77	92
hexyl-**P3**	3.0	75	

[a]Calculated using eq 1. [b]Calculated using eq 2. Peak integrals from ^{29}Si CPMAS NMR spectra were used in all calculations.

3.4. Characterization of Hydrosilylation Efficiency. With the optimized NMR parameters, the ^{29}Si ssNMR spectra could be integrated to estimate the consumption of Si−H residues and conversion to Si−R. The hydrosilylation of each parent polymer **P1**, **P2**, and **P3** led to a decrease in the peaks assigned to the internal Si−H (δ −108) and end group SiH_2 (δ −91) as well as an increase in peaks corresponding to internal functionalized silicon (Si-Hex or Si-Dec, δ −53) and end group ($SiHex_2$ or $SiDec_2$, δ 19) (Figures 5, S7, S8). The assignment of the hexylsilane resonances was made by analogy to the small molecules **2**−**4** and prior work.[20,22,23,26]

Each observed peak was integrated, and the Si−Me resonance (δ = −26 ppm) was normalized to 4Si. The percent functionalization for both internal and end group Si−H bonds was calculated (Table 2). To calculate the percent conversion, the integration of the peak corresponding to the alkylated silicon (either internal or end group) was divided by the sum integration of the peaks corresponding to the alkylated and unalkylated silicon according to eqs 1 and 2.

https://doi.org/10.1021/acs.macromol.3c02110
Macromolecules XXXX, XXX, XXX−XXX

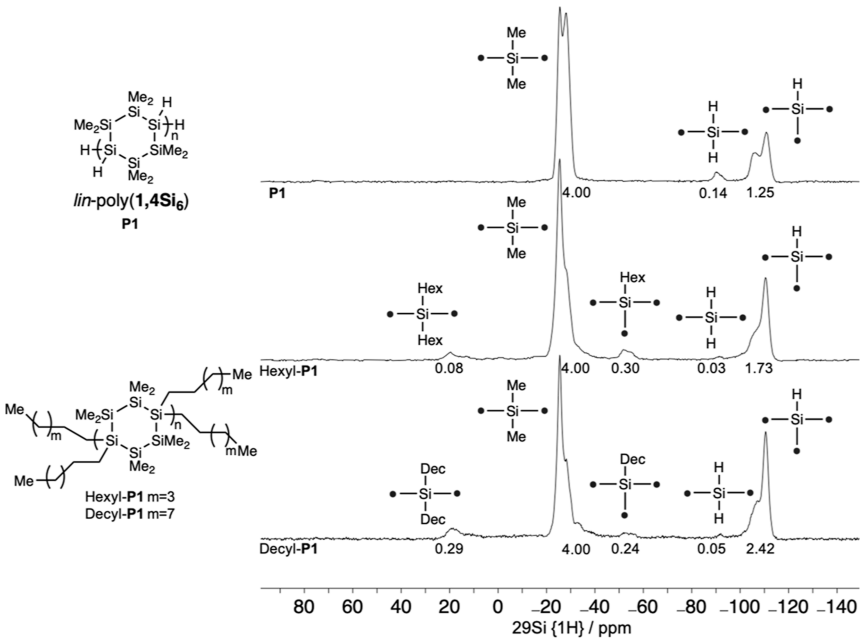

Figure 5. ^{29}Si CPMAS ssNMR (500 MHz) of **P1**, hexyl-**P1**, and decyl-**P1** with peak integrations.

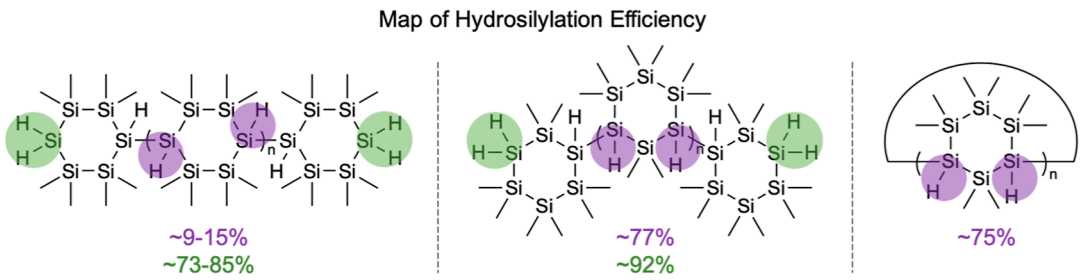

Figure 6. Map of the approximate hydrosilylation efficiency for **P1**, **P2**, and **P3**. End group SiH_2 functionalization is marked in green and internal Si−H functionalization is marked in purple.

$$\frac{\text{Si}-\text{alkyl}}{(\text{Si}-\text{alkyl} + \text{Si}-\text{H})} \times 100 = \text{interal percent functionalization} \quad (1)$$

$$\frac{\text{Si}-\text{alkyl}_2}{(\text{Si}-\text{alkyl}_2 + \text{Si}-\text{H}_2)} \times 100 = \text{end group percent functionalization} \quad (2)$$

To validate the overall accuracy of these estimated conversions measured from ^{1}H−^{29}Si CPMAS ssNMR spectra, we collected a second data set for hexyl-**P2** using the reported quantitative solid-state ^{13}C NMR from a multiple-cross-polarization (multiCP) pulse sequence of Johnson and Schmidt-Rohr.[42] The multiCP pulse sequence has been demonstrated to provide more accurate peak intensities and integrals for both small molecules (e.g., alanine) and complex organic materials such as pyrolysis-derived chars and plant matter. MultiCP incorporates several ^{1}H→^{29}Si CP steps, thus increasing the magnetization transfer to all Si atoms present in the sample, in comparison to CPMAS, in which a single ^{1}H→^{29}Si CP transfer preferentially occurs to Si atoms that are closest in proximity to H atoms. The multiCP experiments were optimized on the **1,4Si$_6$** monomer because it offered much better sensitivity than the polymers. From these experiments, we identified the optimal number of CP steps (3) and the CP contact time (8.0 ms). With the optimized multiCP parameters, we obtained peak integral ratios of 4:2 $SiMe_2$:SiH_2 for the **1,4Si$_6$** monomer. The agreement of the integration values to the number of corresponding silicon environments demonstrates the reliability of the multiCP NMR experiment.

The application of the multiCP pulse program to hexyl-**P2** (Figure S9) resulted in more accurate peak integrals. When the integral of the $SiMe_2$ peak at −26 ppm was set to 4.00, then the sum of all peak integrals was 6.03, consistent with the presence of six Si atoms in the poly(cyclosilane) ring. In comparison, following the same procedure gave a sum of all peak integrals of 5.76 with the ^{29}Si CPMAS pulse sequence. However, calculated percent functionalization using eqs 1 and 2 yielded similar values when peak integrations were used for both NMR methods (Table S2 and Figure S10). Similar percent functionalization was obtained because the relative integrals of the Si-alkyl$_n$ and Si−H$_n$ peaks are approximately the same in the CPMAS and multiCP spectra. Given the shorter data collection times for ^{29}Si CPMAS (ca. 12 h vs 7 days) and the overall agreement between the percent functionalization determined by both NMR methods, multiCP was not applied to the other hydrosilylated polymers.

A map of hydrosilylation efficiency is shown in Figure 6, focusing on the site-selectivity between end groups and

https://doi.org/10.1021/acs.macromol.3c02110
Macromolecules XXXX, XXX, XXX−XXX

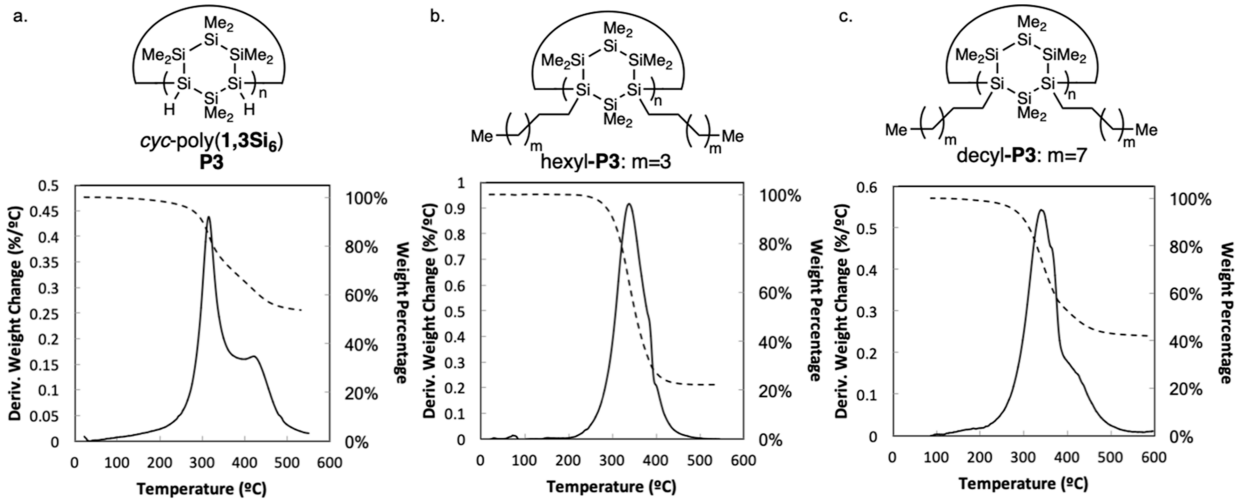

Figure 7. (a–c) TGA curves of **P3**, hexyl-**P3**, and decyl-**P3**. Solid lines: derivative weight change; dotted lines: percentage weight change.

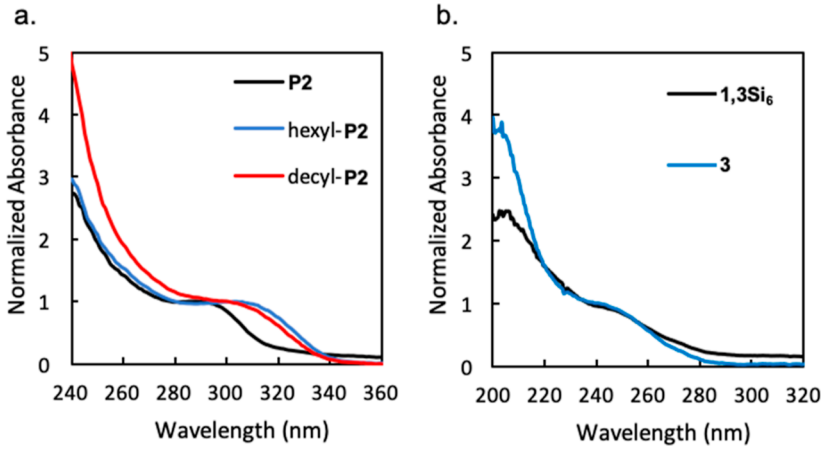

Figure 8. UV–vis spectra of (a) **P2**, hexyl- and decyl-**P2** with normalized absorbance ([compound] = 6.24×10^{-6} M, in THF) and (b) **1,3Si$_6$** and **3** with normalized absorbance ([compound] = 3.00×10^{-5} M, in pentane).

internal sites. Both sites underwent hydrosilylation, as predicted by the small molecule studies, although higher conversions were observed at the less hindered end groups. Although full consumption of all Si–H residues was not achieved, a high degree of functionalization (approximately 75–77%) was achieved with the more soluble polymers **P2** and **P3**. The mostly insoluble **P1** had a high degree of end group functionalization (approximately 73–85%) and low degree of internal functionalization (approximately 9–15%), indicating that the less sterically hindered end groups are more readily reactive or more solvent accessible.

Cyclic hexyl-**P3** showed a high degree of functionalization, in contrast to the observation from GPC that molecular weight characteristics did not change. Not only does this indicate that ^{29}Si CPMAS is a more accurate method of polymer microstructural characterization, it also affirms the unique characteristics of cyclic polymers for GPC. Although it has been demonstrated that ^{29}Si CPMAS was not applied to decyl-**P2** and decyl-**P3** due to their oily nature, it is reasonable to assume similar reactivity for 1-hexene and 1-decene in the hydrosilylation reactions given their similar structures.

3.5. Impact of Postpolymerization Functionalization on Physical Properties. Complementing structural characterization by NMR spectroscopy, we sought to understand how alkylation might influence the physical properties of the poly(cyclosilane)s. We focused on several key properties of polysilanes: their pyrolysis to silicon carbide, UV–vis light absorption, and susceptibility to oxidation via Si–H autoxidation.

3.5.1. Pyrolysis. It is known that polysilanes such as poly($SiMe_2$) form silicon carbide (SiC) upon pyrolysis via Kumada rearrangement of the polysilane to a polycarbosilane, followed by cross-linking.[29,43] In prior work investigating the thermal properties of the hydrido-terminated poly(cyclosilane)s, we found two stages of thermal decomposition by TGA (Figure 7a), which were attributed to Si–Si bond cleavage (200–350 °C) followed by side chain rearrangement and cross-linking (350–500 °C).[27] Char yields between 50 and 60% were observed. It has been hypothesized that Si–H side chains facilitate interchain covalent cross-linking (e.g., thermosetting),[44] thereby increasing the char yields of SiC. If so, we would expect hydrosilylation, which consumes Si–H bonds, to decrease char yields and predominantly influence pyrolytic cross-linking occurring in the 350–500 °C temperature range.

TGA was performed on **P1–3** and their alkylated variants to compare thermal decomposition when heated from 40 to 600 °C in an argon flow. As shown for **P3**, hexyl-**P3**, and decyl-**P3**

https://doi.org/10.1021/acs.macromol.3c02110
Macromolecules XXXX, XXX, XXX–XXX

as representative samples, we observed a reduction in the overall char yield from 55% (Figure 7a) to 20% (Figure 7b) and 40% (Figure 7c) after hydrosilylation. The onset of thermal decomposition was the same as that for the parent structure **P3** (200−350 °C); however, the second phase of pyrolysis was markedly less pronounced, as is particularly clear in the derivative weight change curves (solid lines). Similar trends were observed for **P1** and **P2** (Figures S11 and S12). The pyrolytic reactivity is therefore consistent with the attachment of alkyl chains to the poly(cyclosilane) skeleton.

3.5.2. UV−Vis Absorbance Spectra. We obtained UV−vis absorption spectra of the alkyl-functionalized poly(cyclosilane)s. As the chromophore in the poly(cyclosilane)s is the σ-conjugated skeleton, if hydrosilylation occurred with concomitant Si−Si scission, we would observe a blue shift in the absorption spectrum. Instead, we observed an intriguing 20 nm red shift of the absorption band for the functionalized polymers hexyl- and decyl-**P2** (λ_{max} = 310 nm) relative to the parent polymer **P2** (λ_{max} = 292 nm). A similar shift was observed for **P3** (from λ_{max} = 296 to 314 nm, Figure S13) and a less prominent shift was observed for **P1** (from λ_{max} = 271 to ∼274 nm, Figure S14). The red shift is intriguing as the alkyl chains should not engage in resonance delocalization with the Si−Si framework. Indeed, a comparison of the UV−vis spectra of **1,3Si$_6$** and tetra-alkylated cyclosilane **3** (synthesized via a hydrosilylation reaction between **1,3Si$_6$** and excess 1-hexene) showed no difference in their absorption spectra (Figure 8b).

The observed bathochromic shift upon attachment of long alkyl side chains is reminiscent of Miller's seminal studies of thermochromism in poly(Si(*n*-hex)$_2$), in which reversible side chain crystallization induced a change in the polysilane backbone conformation from disordered to all-*anti* with an accompanying change in λ_{max} from 317 to 370 nm.[45,46] We therefore hypothesize that the hexyl and decyl chains contributed to a change in the poly(cyclosilane) conformation that maximizes light absorption.

3.5.3. Si−H Autoxidation. IR spectroscopy gave insight into how the conversion of Si−H bonds to Si−C bonds affected air stability and decreased the level of silane autoxidation. Increased stability against oxidation was clearly demonstrated with the functionalized small molecules **2**−**4**. Samples were exposed to air on the benchtop for 7 days or exposed to air while refluxing in xylenes for 24 h. The results of both methods were monitored via IR spectroscopy (Figures 9, S15, and S16) to observe any relative differences in the Si−O stretch (1100 cm^{-1}) relative to those of unoxidized samples. The H-functionalized cyclosilanes, as exemplified by **1,4Si$_6$** (Figure 9a), showed a significant Si−O stretch after benchtop storage and an even more pronounced feature after reflux in xylenes in air. Compounds **2**−**4** that lacked Si−H bonds changed minimally in the Si−O region when stored on the benchtop at room temperature, speaking to the protective effect of Si−H for Si−R replacement. Similar increases in air stability have been observed for alkyl-terminated silicon nanoparticles.[47] However, some oxidation was still observed at higher temperatures, although less than that for the H-functionalized small molecules. Since the functionalized polymers did not reach 100% conversion of Si−H side chains to Si−R, alkylation reduced the rate of oxidation as compared to **P1**-**3** (Figure S17−S19), but Si−O was still eventually observed.

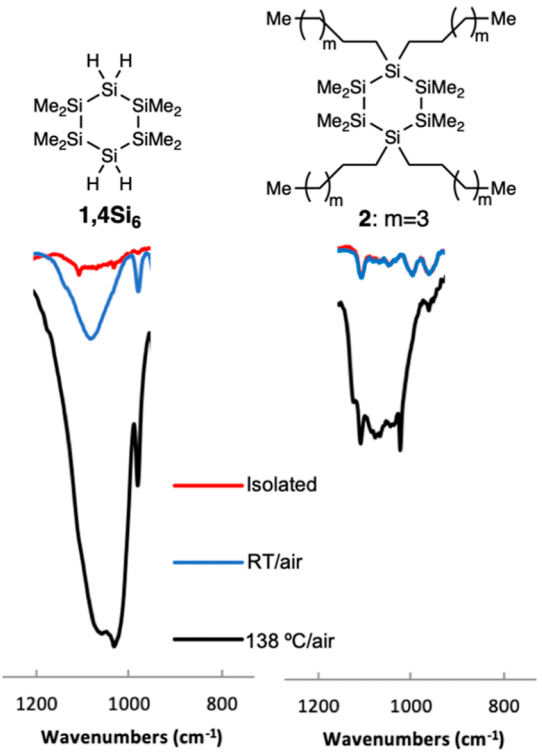

Figure 9. Cropped IR spectra, Si−O region of **1,4Si$_6$** and **2**.

4. CONCLUSIONS

We have investigated the postpolymerization functionalization of poly(cyclosilane)s **P1**−**3** via a borane-catalyzed hydrosilylation reaction between the H-functionalized polymers and simple α-olefins. Evidence for the high reactivity and chemoselectivity of the catalyst emerged from studies on molecular analogues of the complex polymers. Structural characterization of the alkylated poly(cyclosilane)s via FTIR spectroscopy was consistent with the consumption of Si−H residues and conversion to Si−R residues. GPC analysis, however, provided inconsistent data with respect to changes in molecular weight characteristics, indicating a need for more precise characterization tools. We employed ssNMR spectroscopy to characterize the site selectivity and overall conversion of poly(cyclosilane) functionalization, which were typically >75%.

The attachment of long alkyl chains to the polysilanes resulted in significant changes in solubility, air stability, thermal decomposition, and, surprisingly, their UV−vis absorbance spectra. The discovery of catalysts effective for even high levels of conversion might result in benchtop-stable poly(cyclosilane)s by replacement of the Si−H side chains prone to autoxidation with less reactive Si−R side chains. Future studies will investigate the relationship among side chain structure, macromolecular conformation, and light absorption as well as opportunities for higher degrees of functionalization.

■ ASSOCIATED CONTENT

Supporting Information

The Supporting Information is available free of charge at https://pubs.acs.org/doi/10.1021/acs.macromol.3c02110.

Poly(cyclosilane) postpolymerization hydrosilylation raw NMR FIDs (ZIP)

https://doi.org/10.1021/acs.macromol.3c02110
Macromolecules XXXX, XXX, XXX−XXX

Supplemental figures and characterization data (NMR, SEC, TGA, and IR) (PDF)

AUTHOR INFORMATION

Corresponding Author

Rebekka S. Klausen − *Department of Chemistry, Johns Hopkins University, Baltimore, Maryland 21218, United States;* orcid.org/0000-0003-4724-4195; Email: klausen@jhu.edu

Authors

Marissa G. Coschigano − *Department of Chemistry, Johns Hopkins University, Baltimore, Maryland 21218, United States*

Sydney L. Gregory − *Department of Chemistry, Johns Hopkins University, Baltimore, Maryland 21218, United States*

Jonathan Catazaro − *Department of Chemistry, Johns Hopkins University, Baltimore, Maryland 21218, United States*

Aaron J. Rossini − *Department of Chemistry, Iowa State University, Ames, Iowa 50011, United States; US DOE Ames National Laboratory, Ames, Iowa 50011, United States;* orcid.org/0000-0002-1679-9203

Complete contact information is available at: https://pubs.acs.org/10.1021/acs.macromol.3c02110

Notes

The authors declare no competing financial interest.

ACKNOWLEDGMENTS

This research was primarily supported by the U.S. Department of Energy (DOE), Office of Science, Basic Energy Sciences, under award no. DE-SC0020681. CP-MAS spectroscopy was made possible through the National Science Foundation Major Research Instrumentation grant CHE-2018176.

REFERENCES

(1) Kipping, F. S. CCCVIII.—Organic Derivatives of Silicon. Part XXX. Complex Silicohydrocarbons $[SiPh_2]_N$. *J. Chem. Soc., Dalton Trans.* **1924**, *125* (0), 2291−2297.

(2) Klausen, R. S.; Ballestero-Martínez, E. Organosilicon and Related Group 14 Polymers Parkin, G., Meyer, K., O'Hare, D., Eds.; Elsevier, 2022, pp 135−165.*Comprehensive Organometallic Chemistry IV*

(3) Miller, R. D.; Michl, J. Polysilane High Polymers. *Chem. Rev.* **1989**, *89* (6), 1359−1410.

(4) Marro, E. A.; Klausen, R. S. Conjugated Polymers Inspired by Crystalline Silicon. *Chem. Mater.* **2019**, *31* (7), 2202−2211.

(5) Koe, J.; Fujiki, M. *Organosilicon Compounds*; Elsevier, 2017, pp 219−300.Polysilanes

(6) Maxka, J.; Mitter, F. K.; Powell, D. R.; West, R. Assignment of Configuration in Phenylmethylpolysilanes. *Organometallics* **1991**, *10* (3), 660−664.

(7) Fossum, E.; Matyjaszewski, K. Ring-Opening Polymerization of Cyclotetrasilanes: Microstructure and Mechanism. *Macromolecules* **1995**, *28* (5), 1618−1625.

(8) Jones, R. G.; Benfield, R. E.; Evans, P. J.; Holder, S. J.; Locke, J. A. M. A Reappraisal of the Stereochemistry of Polysilylenes Formed by the Wurtz Reductive-Coupling Reaction. *J. Organomet. Chem.* **1996**, *521* (1−2), 171−176.

(9) Herzog, U.; West, R. Heterosubstituted Polysilanes. *Macromolecules* **1999**, *32* (7), 2210−2214.

(10) Uhlig, W. Zur Synthese Funktionel Substituierter Polysilane Mittels Trifluormethansulfonsäure. *J. Organomet. Chem.* **1991**, *402* (3), C45−C49.

(11) Carberry, E. A.; West, R. Cyclic Polysilanes. III. Preparation of Permethylcyclopolysilanes by Coupling, Pyrolysis, and Redistribution Reactions. *J. Am. Chem. Soc.* **1969**, *91* (20), 5440−5446.

(12) Matyjaszewski, K.; Hrkach, J. S. Modification of Polysilanes: Preparation of Comb-like Graft Copolymers. *J. Inorg. Organomet. Polym.* **1995**, *5* (2), 183−193.

(13) Aitken, C.; Harrod, J. F.; Gill, U. S. Structural Studies of Oligosilanes Produced by Catalytic Dehydrogenative Coupling of Primary Organosilanes. *Can. J. Chem.* **1987**, *65* (8), 1804−1809.

(14) Woo, H. G.; Walzer, J. F.; Tilley, T. D. Sigma.-Bond Metathesis Mechanism for Dehydropolymerization of Silanes to Polysilanes by D0Metal Catalysts. *J. Am. Chem. Soc.* **1992**, *114* (18), 7047−7055.

(15) Banovetz, J. P.; Hsiao, Y. L.; Waymouth, R. M. Selective Free-Radical Halogenation of Polyphenylsilane. *J. Am. Chem. Soc.* **1993**, *115* (6), 2540−2541.

(16) Liu, H. Q.; Harrod, J. F. Dehydrocoupling of Ammonia and Silanes Catalyzed by Dimethyltitanocene. *Organometallics* **1992**, *11* (2), 822−827.

(17) Kato, N.; Tamura, Y.; Kashiwabara, T.; Sanji, T.; Tanaka, M. AlCl3-Catalyzed Hydrosilylation of Alkynes with Hydropolysilanes. *Organometallics* **2010**, *29* (21), 5274−5282.

(18) Harrison, D. J.; Edwards, D. R.; McDonald, R.; Rosenberg, L. Toward Selective Functionalisation of Oligosilanes: Borane-Catalysed Dehydrogenative Coupling of Silanes with Thiols. *Dalton Trans.* **2008**, No. 26, 3401−3411.

(19) Lee, P. T. K.; Skjel, M. K.; Rosenberg, L. Borane-Catalyzed Si-H Activation Routes to Polysilanes Containing Thiolato Side Chains. *Organometallics* **2013**, *32* (6), 1575−1578.

(20) Lee, P. T. K.; Rosenberg, L. Borane-Catalysed Postpolymerisation Modification of the Si-H Bonds in Poly(Phenylsilane). *Dalton Trans.* **2017**, *46* (27), 8818−8826.

(21) Marro, E. A.; Klausen, R. S. Conjugated Polymers Inspired by Crystalline Silicon. *Chem. Mater.* **2019**, *31* (7), 2202−2211.

(22) Press, E. M.; Marro, E. A.; Surampudi, S. K.; Siegler, M. A.; Tang, J. A.; Klausen, R. S. Synthesis of a Fragment of Crystalline Silicon: Poly(Cyclosilane). *Angew. Chem., Int. Ed.* **2017**, *56* (2), 568−572.

(23) Marro, E. A.; Press, E. M.; Siegler, M. A.; Klausen, R. S. Directional Building Blocks Determine Linear and Cyclic Silicon Architectures. *J. Am. Chem. Soc.* **2018**, *140* (18), 5976−5986.

(24) Folster, C. P.; Klausen, R. S. Metallocene Influence on Poly(Cyclosilane) Structure and Properties. *Polym. Chem.* **2018**, *9* (15), 1938−1941.

(25) Jiang, Q.; Gittens, A. F.; Wong, S.; Siegler, M. A.; Klausen, R. S. Highly Selective Addition of Cyclosilanes to Alkynes Enabling New Conjugated Materials. *Chem. Sci.* **2022**, *13* (25), 7587−7593.

(26) Dorn, R. W.; Marro, E. A.; Hanrahan, M. P.; Klausen, R. S.; Rossini, A. J. Investigating the Microstructure of Poly(Cyclosilane) by 29Si Solid-State NMR Spectroscopy and DFT Calculations. *Chem. Mater.* **2019**, *31* (21), 9168−9178.

(27) Jiang, Q.; Wong, S.; Klausen, R. S. Effect of Polycyclosilane Microstructure on Thermal Properties. *Polym. Chem.* **2021**, *12* (33), 4785−4794.

(28) Fang, F.; Jiang, Q.; Klausen, R. S. Poly(Cyclosilane) Connectivity Tunes Optical Absorbance. *J. Am. Chem. Soc.* **2022**, *144* (17), 7834−7843.

(29) Ackley, B. J.; Martin, K. L.; Key, T. S.; Clarkson, C. M.; Bowen, J. J.; Posey, N. D.; Ponder Jr, J. F.; Apostolov, Z. D.; Cinibulk, M. K.; Pruyn, T. L.; Dickerson, M. B. Advances in the Synthesis of Preceramic Polymers for the Formation of Silicon-Based and Ultrahigh-Temperature Non-Oxide Ceramics. *Chem. Rev.* **2023**, *123* (8), 4188−4236.

(30) Chatgilialoglu, C.; Guerrini, A.; Lucarini, M.; Pedulli, G. F.; Carrozza, P.; Da Roit, G.; Borzatta, V.; Lucchini, V. Autoxidation of Poly(Hydrosilane)S. *Organometallics* **1998**, *17* (11), 2169−2176.

(31) Buriak, J. M. Organometallic Chemistry on Silicon and Germanium Surfaces. *Chem. Rev.* **2002**, *102* (5), 1271−1308.

(32) Ohshita, J.; Matsuzawa, Y.; Yagami, T.; Adachi, Y.; Sekiguchi, A.; Ohashi, M.; Nakano, H. Photo-Energy Transfer in σ-π Conjugated

Polysilanes Prepared by Platinum-Catalyzed Reactions of Arylacetylenes with Layered Polysilane. *Chem. Lett.* **2020**, *49* (10), 1174−1177.
(33) Purkait, T. K.; Iqbal, M.; Wahl, M. H.; Gottschling, K.; Gonzalez, C. M.; Islam, M. A.; Veinot, J. G. C. Borane-Catalyzed Room-Temperature Hydrosilylation of Alkenes/Alkynes on Silicon Nanocrystal Surfaces. *J. Am. Chem. Soc.* **2014**, *136* (52), 17914−17917.
(34) Fischer, R.; Konopa, T.; Ully, S.; Baumgartner, J.; Marschner, C. Route Si6 Revisited. *J. Organomet. Chem.* **2003**, *685* (1−2), 79−92.
(35) Bennett, A. E.; Rienstra, C. M.; Auger, M.; Lakshmi, K. V.; Griffin, R. G. Heteronuclear Decoupling in Rotating Solids. *J. Chem. Phys.* **1995**, *103* (16), 6951−6958.
(36) Wang, T. W.; Golder, M. R. *Polymer Chemistry*.; Royal Society of Chemistry, 2021, pp 958−969.Advancing Macromolecular Hoop Construction: Recent Developments in Synthetic Cyclic Polymer Chemistry
(37) Roland, C. D.; Li, H.; Abboud, K. A.; Wagener, K. B.; Veige, A. S. Cyclic Polymers from Alkynes. *Nat. Chem.* **2016**, *8* (8), 791−796.
(38) Bovey, F. A.; Tiers, G. V. D.; Filipovich, G. Polymer NSR Spectroscopy. I. The Motion and Configuration of Polymer Chains in Solution. *J. Polym. Sci.* **1959**, *38* (133), 73−90.
(39) Spiess, H. W. *50th Anniversary Perspective*: The Importance of NMR Spectroscopy to Macromolecular Science. *Macromolecules* **2017**, *50* (5), 1761−1777.
(40) Miyoshi, T. *Molecular Characterization of Polymers: A Fundamental Guide*; Elsevier, 2021, pp 409−440.Characterization of Polymers by NMR
(41) Alemany, L. B.; Grant, D. M.; Pugmire, R. J.; Alger, T. D.; Zilm, K. W. Cross Polarization and Magic Angle Sample Spinning NMR Spectra of Model Organic Compounds. 2. Molecules of Low or Remote Protonation. *J. Am. Chem. Soc.* **1983**, *105* (8), 2142−2147.
(42) Johnson, R. L.; Schmidt-Rohr, K. Quantitative Solid-State 13C NMR with Signal Enhancement by Multiple Cross Polarization. *J. Magn. Reson.* **2014**, *239*, 44−49.
(43) Yajima, S.; Hasegawa, Y.; Okamura, K.; Matsuzawa, T. Development of High Tensile Strength Silicon Carbide Fibre Using an Organosilicon Polymer Precursor. *Nature* **1978**, *273* (5663), 525−527.
(44) Zhang, Z.-F.; Babonneau, F.; Laine, R. M.; Mu, Y.; Harrod, J. F.; Rahn, J. A. Poly(Methylsilane)-A High Ceramic Yield Precursor to Silicon Carbide. *J. Am. Ceram. Soc.* **1991**, *74* (3), 670−673.
(45) Miller, R. D.; Hofer, D.; Rabolt, J.; Fickes, G. N. Anomalously Long-Wavelength Electronic Transition in Conformationally Locked Organosilane High Polymers. *J. Am. Chem. Soc.* **1985**, *107* (7), 2172−2174.
(46) Rabolt, J. F.; Hofer, D.; Miller, R. D.; Fickes, G. N. Studies of Chain Conformational Kinetics in Poly(Di-n-Alkylsilanes) by Spectroscopic Methods. 1. Poly(Di-n-Hexylsilane), Poly(Di-n-Heptylsilane), and Poly(Di-n-Octylsilane). *Macromolecules* **1986**, *19* (3), 611−616.
(47) Yang, C. S.; Bley, R. A.; Kauzlarich, S. M.; Lee, H. W. H.; Delgado, G. R. Synthesis of Alkyl-Terminated Silicon Nanoclusters by a Solution Route. *J. Am. Chem. Soc.* **1999**, *121* (22), 5191−5195.

https://doi.org/10.1021/acs.macromol.3c02110
Macromolecules XXXX, XXX, XXX−XXX